Microstructure and Solidification of Al-Fe-(V, Si) Alloy Powders

Ruangdaj Tongsri,[a,*] **Richard Dashwood**[b] **and Henry Mcshane**[b]

[a] National Metal and Materials Technology Center (MTEC), Thailand Science Park, 114 Paholyothin Rd., Klong 1, Klong Luang, Phatumthani 12120 Thailand
[b] Department of Materials, Imperial College of Science, Technology and Medicine, Prince Consort Rd., London SW7 2 BP, UK.

* Corresponding author, E-mail: ruangdt@mtec.or.th

Abstract: Gas-atomised powders of Al-Fe-(V, Si) alloys exhibited microstructures consisting of cells and/or some forms of icosahedral phase. The forms of icosahedral phase include irregular shaped aggregates of ultrafine spherical micro-quasicrystalline (MI) particles in α–aluminium phase matrix, ultrafine MI particles in intercellular regions, and globular clusters of randomly oriented MI particles (in medium to coarse size Al-Fe-V alloy powders) or globular particles of single icosahedral phase (in medium to coarse size Al-Fe-V-Si alloy powders). It has been proposed that solidification behavior of the Al-Fe-(V, Si) alloy powders would be attributed to a competition between growth of α–aluminium phase fronts and freely nucleated icosahedral particles. Interactions between the solidification fronts and dispersed particles, influenced by solidification rates, would control microstructural morphology.

Keywords: microstructure, solidification, gas-atomised powders. Al-Fe-(V, Si) alloys.

Introduction

Rapidly solidified Al-Fe alloy systems have been considered as potential candidates for production of lightweight alloys with useful mechanical properties at elevated temperatures. This is attributed to fact that this type of materials has good microstructural stability due to precipitation strengthening by stable refined Al-Fe intermetallics. Solubility of Fe in Al is very limited when the alloy is produced using conventional solidification methods with slow cooling rates and hence slow solidification rates. Therefore, precipitation strengthening which enhances the material's strength is limited due to several factors, such as large particle size, low volume fraction, and inhomogeneous distribution of Al-Fe intermetallics. However, it has been discovered that using rapid solidification methods could extend solubility of Fe in Al. In addition to extended solubility of alloying elements, other effects such as microstructure refinement, chemical homogeneity, and formation of metastable phases, are also produced by rapid solidification.

Microstructures of rapidly solidified Al-Fe alloys are the results of solidification behaviours of the solidifying fronts growing into the melt and of primary intermetallic phases distributed in the melt. Most rapidly solidified Al-Fe alloys exhibited cellular growth of the solidifying fronts.[1-5] Microstructures of splat-cooled binary Al-Fe alloys exhibited two features.[1] The first structure was designated as 'zone A', which referred to a cellular or dendritic-like structure with an arm spacing of ~300 angstrom in colonies of ~1 mm in diameter. The second structure was designated as 'zone B', which referred to a coarser background network structure in which primary intermetallic particles (Al_6Fe) ~1 mm apart act as growth centers.

Formation of primary intermetallic phases in rapidly solidified hyper-eutectic Al-Fe alloys with up to 35 wt. % Fe has been widely investigated. These phases included primary α–Al, Al_3Fe, Al_6Fe, Al_mFe, quasi-crystalline phases (decagonal and icosahedral), and intercellular/dendritic phases which could be Al_6Fe, Al_mFe or quasi-crystalline phases, depending on the cooling rate and the alloy composition. Before 1984, both the globular phases and the phases at the cell walls formed in rapidly solidified Al-Fe alloys were reported as being the same 'S' phase.[6] However, since the discovery of the icosahedral phase in rapidly solidified Al-Mn,[7] the independently nucleating spherical primary particles possessing electron diffraction patterns with typical icosahedral symmetry, referred to as an 'O' phase, have been identified as icosahedral phase particles in the Al-Fe system.[8] The formation of icosahedral phase particles was claimed to result from diffusionless solidification with growth rates of 1-2 m/s.

Melt-spun Al-Fe alloys containing up to 15 wt. % Fe

were observed to solidify with microcellular structures, and the intercellular phases were later identified as unoriented micro-quasicrystals.[9] Al_6Fe was also reported to be present at grain boundaries in slowly cooled regions in these alloys. Microstructures consisting of quasi-crystalline phases are typical in rapidly solidified Al-Fe alloys containing 15-22 wt. %Fe. The presence of icosahedral phases in these alloys has been reported by several researchers.[7,8] However, the presence of the icosahedral phases in rapidly solidified Al-Fe alloys is a subject of controversy. It has been reported that decagonal phases exist in rapidly solidified Al-Fe alloys rather than icosahedral phases.[10] The Al_mFe phase was found to exist in both forms of primary Al_mFe particles and α-Al-Al_mFe eutectic in melt-spun Al-10 at. %(19 wt. %)Fe.[10] In rapidly solidified Al-Fe alloys containing 25-35 wt. %Fe, microstructures were reported to contain primary $Al_{13}Fe_4$ showing a radial array of heavily twinned $Al_{13}Fe_4$ dendritic branches.[8,10] There was close similarity between electron diffraction patterns of the decagonal, Al_mFe, and $Al_{13}Fe_4$ phases,[10] suggesting that the $Al_{13}Fe_4$, and Al_mFe phases may be approximants of the Al-Fe decagonal phase.

In the early stage of development, investigations of the rapidly solidified Al-Fe-V alloy system (8 to 14 wt. %Fe, and 1 to 3.5 wt. %V)[11] using the melt-spinning technique showed that microstructures of the as-cast products consist of zone A and zone B, and the extent of both zones depends on the processing parameters, namely, surface velocity of casting or wheel speed. The as-cast microstructures of melt-spun Al-Fe-V-Si alloys[12] have been reported to vary depending on casting conditions and also through the thickness of the ribbon. Two types of alloy ribbons have been found in the melt-spun Al-8.5Fe-1.3V-1.7Si alloy.[12] The first type was completely zone A ribbon in which microquasi-crystalline phase precipitated in intercellular regions. The second type was mixed zone A and zone B ribbon in which silicide phase, transformed from microquasi-crystalline phase due to recalescence, was observed in intercellular regions. In both cases, globular particles of clustered microquasi-crystalline phase were present near the air side of the ribbons. The globular particles of clustered microquasi-crystalline phase and the intercellular microquasi-crystalline phase were claimed to nucleate prior to the formation of aluminium cells.[12]

Microstructural evolution in melt-spun alloy with a composition of $Al_{80}Fe_{10}V_{10}Si_6$ was reported to be slightly different, particularly in the regions where quasi-crystalline phases formed.[13] A crystalline ring of small cubic-structure silicide particles has been observed to surround a quasi-crystalline phase. Decomposition of the quasi-crystalline phase resulted in formation of polycrystalline aggregates of cubic crystals with irrational twinning leading to icosahedral symmetry in

reciprocal space. Recently, melt-spun $Al_{93.3}Fe_{4.3}V_{0.7}Si_{1.7}Mm_x$ ($x = 0.5, 1, 3$), where Mm = 55Ce, 29La, 11Nd, and 5Pr (wt. %), has been found to exhibit different microstructures from the well known melt-spun Al-Fe-V-Si alloys.[14] For $x = 0.5$, the microstructure consisted of mixed phases of α–$Al_{13}(Fe, V)_3Si_1$, and Al_8Fe_4Mm. Only Al_8Fe_4Mm phase was observed in the microstructure for $x = 1$, whereas quasi-crystalline $Al_{20}Fe_5Mm$ phase was identified for $x = 3$.

In this investigation, results of microstructural characterisation of the rapidly solidified Al-Fe-(V, Si) alloy powders are reported. Explanation for the microstructural development is given with comparison to other works.[1-22] The solidification mechanism of the powders is also proposed using interactions between the solidification fronts and dispersed particles.[23-25]
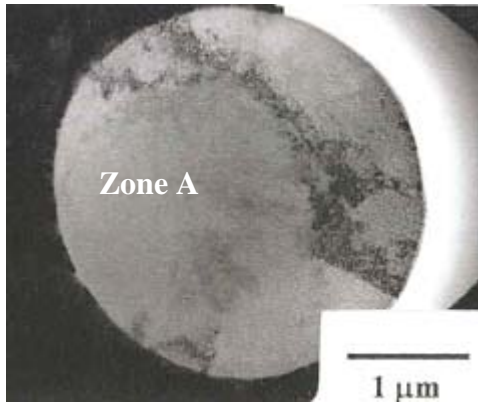
MATERIALS AND METHODS

Gas-atomised powders of Al-6.5Fe-1.5V (alloy X) and Al-6.5Fe-1.5V-1.7Si (alloy Y) were supplied by ALPOCO, UK. The nominal compositions of the powders investigated in this paper referred to chemical analysis performed by the powder supplier. Microstructures of the alloy X and alloy Y powders were investigated using transmission electron microscopy (TEM), on a JEOL-FX2000EM, equipped with energy dispersive X-ray spectroscopy (EDS), and a LINK X-ray Analytical System, operating at 200kV. TEM specimen preparation for the powders was carried out using the following steps. In the first step, the powders were embedded in a nickel foil. This could be done by placing the powders on a steel cathode immersed in a nickel ion-containing electrolyte of an electrolysis unit. With appropriate electric potential and current, nickel ion would be reduced and deposited on the cathode surface and hence the powders were embedded in the deposited nickel. Then, the embedded nickel foil was ground until its thickness was less than 100 mm. In the next step, a disc with diameter of 3 mm was made from the thin foil. Finally, the disc was thinned electrolytically using a Struers Tenupol jet polishing machine, with a solution (by volume) of 10% percholic acid, 10% 2-butoxyethanol, and 80% ethanol, operating at −35°C and 65 V.
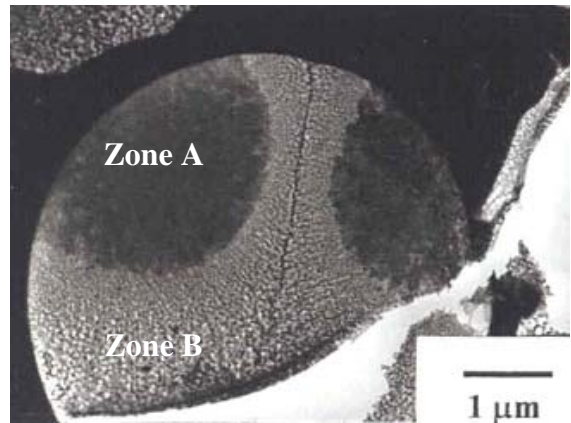
RESULTS AND DISCUSSION
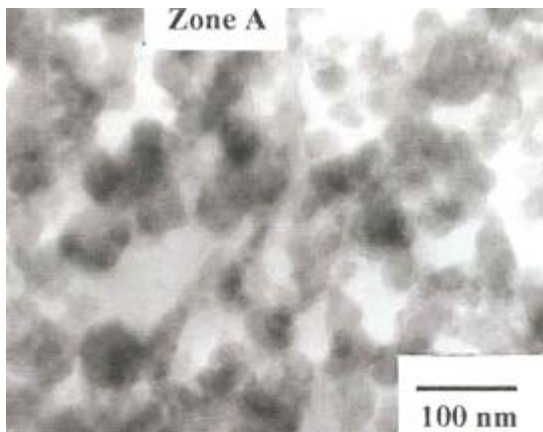
Microstructure of Fine Size Powders (< 5 µm)

Observation using TEM revealed the microstructural morphologies of alloys X and Y powders. Microstructural morphology of the powders depended on powder particle size. Fine size powder particles with diameters of up to 5 µm exhibited ultrafine microstructures (Fig 1a). TEM with higher magnificα–
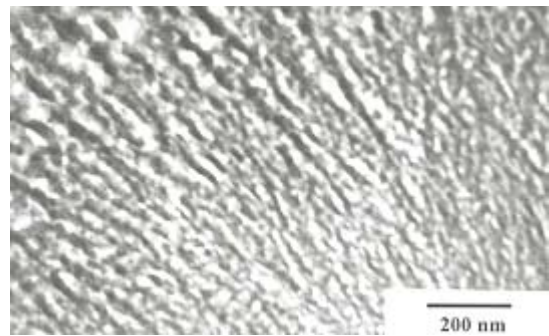
a   A powder particle of alloy X
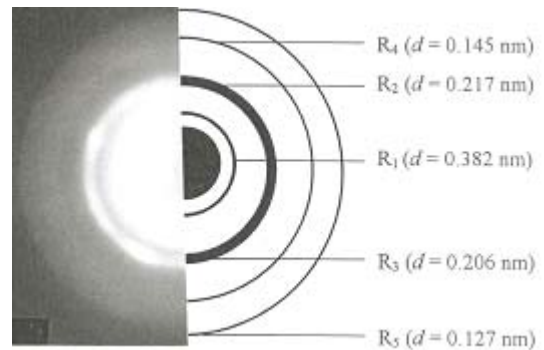

b   Zone A in a powder particle of alloy X

c   SADP of zone A in a powder particle of alloy X

Fig 1. Microstructure of a fine powder particle with size < 5 mm.

a   An alloy Y powder particle

b   Zone B in an alloy Y powder particle

c   SADP of zone B in an alloy Y powder particle

Fig 2. Characteristics of powders with a diameter range of 5-15 mm.

tion revealed that the microstructure consisted of ultrafine, discrete rounded particles with diameters less than 50 nm distributed throughout the α–Al matrix (Fig 1b). This microstructure was obviously different from the microcellular structure shown in Fig 2b. Selected area electron diffraction patterns (SADP) of the area consisting of ultrafine, discrete rounded particles in both alloys X and Y powders exhibited diffuse rings and some diffracted spots from aluminium (Fig 1c).

In previous investigations on splat-quenched Al-Fe[1] and melt-spun Al-Fe[2] alloys, the microstructures consisting of microcells have been designated as 'zone A', whereas the microstructures consisting of coarse and segregated dendrites have been designated as 'zone B'. However, in order to distinguish the microstructure consisting of ultrafine, discrete rounded particles

distributed homogeneously in the α–Al matrix (Fig 1b) from the microstructure consisting of microcells with intercellular particles (Fig 2b), 'zone A' is designated for the former microstructure and 'zone B' is designated for the latter. Microstructures consisting of ultrafine particles randomly oriented in the matrix (similar to zone A designated in this report) have also been reported in melt-spun Al-Fe[2], Al-Fe-Ni[3], and Al-Fe-Mo-V[4] alloys.

Formation of Zone A

Formation of zone A is not well understood. Explanations for formation of zone A have been given by some authors.[2,3] Chu and Granger[2] suggested that the formation of fine particles in zone A microstructures of melt-spun binary Al-Fe alloys was attributed to segregation during solidification rather than solid-state decomposition after solidification because of their random orientation with respect to the α–Al matrix.

Boettinger *et al*[3] found that the morphological transition of the intercellular phases occurred according to solidification velocity in rapidly solidified Al-Fe-Ni alloy. They reported that the intercellular phase morphology changed from continuous forms at low velocities to discrete rounded particles at high velocities. A mechanism for the occurrence of round particles at high velocities involves the formation and subsequent solidification of the isolated droplets of solute-rich liquid within the α–Al matrix. The droplets are formed by a pinching-off of liquid in the grooves in a cellular liquid/solid interface.

The formation of zone A may be explained by considering the interaction between the solidification fronts and freely dispersed particles.[23-25] Before discussing the formation of zone A, it is worth identifying the ultrafine, discrete rounded particles present in the α–Al matrix. These particles forming in the melt droplets may be one of three phases, namely, the amorphous phase, the Frank-Kasper phase and the quasi-crystalline phase.[15] These phases are likely to be present in the solid state to preserve the icosahedral nearest-neighbour co-ordination i.e. a short-range order exhibited by metallic melts.[15] SADPs with a diffuse ring as shown in Fig. 1c may lead to the conclusion that the ultrafine, discrete rounded particles in zone A are an amorphous phase (a normal metallic glass). However, it has been speculated that an SADP with diffuse rings may result from a 'special amorphous phase, which is not a normal metallic glass (dense random packing model), but an orientationally disordered microquasi-crystalline phase.[16]

In a melt-spun Al-Fe-Mo-V ribbon[8], a microstructure consisting of ultrafine and uniformly distributed particles in an α–Al matrix (similar to zone A of the powders investigated in this study) also exhibited an SADP with diffuse rings. When convergent beam

electron diffraction (CBED) was performed on a single ultrafine particle, an SDAP with fivefold symmetry, which is a common feature of the icosahedral phase, was obtained. Owing to the reasons given above, it is speculated that the ultrafine particles in zone A of alloy X and alloy Y powders could be microquasi-crystalline phases. The presence of microquasi-crystalline icosahedral (MI) phases in zone B of alloy Y powder particles may also lead to the speculation that the ultrafine particles in zone A could be MI phase particles.

The formation of zone A may occur by the following mechanisms. After a melt droplet has been highly undercooled, nucleation events of the MI phase particles occur throughout an alloy melt droplet, whereas the nucleation events for stable Al_6Fe and equilibrium $Al_{13}Fe_4$ are suppressed. After nucleation, the MI phase particles grow further and disperse in the melt. At nearly the same time as nucleation of MI phase occurs, nucleation of the α–Al phase begins at the surface of an alloy melt droplet. After this, nucleation the α–Al front advances with a planar front into the melt. In rapid solidification, the planar front velocities are extremely high[5,17] and this is so for the solidification velocities of the α–Al front in small powder particles (although the velocities cannot be experimentally determined during solidification of metal powders). Because of the high solidification front velocities, the ultrafine dispersed MI phase particles are engulfed. This particle engulfment by a planar or a smooth solidification front is illustrated schematically in Fig 3a.

The segregation-free solid could be observed in neither alloy X nor alloy Y powders. The reason for the absence of segregation-free microstructures in these two alloys may be attributed to the formation of the MI phase particles as explained above. The formation of segregation-free solid from the melt in the Al-Fe alloy system is determined by solute trapping at all concentrations.[18] A very high velocity is required to initiate solute trapping in the Al-Fe alloy system. Recently, the solid-liquid interface velocity required for Al-Fe alloys to solidify with a planar front during rapid solidification was experimentally measured using a laser surface treatment.[5] With increasing growth velocity, the microstructures of low Fe containing Al-Fe alloys (with < 0.5 wt. % Fe) were observed to transform from dendritic to banded and finally to precipitation-free. The growth rates required for transition from banded to precipitation-free microstructure were found to increase with increasing alloy content. In higher Fe content Al-Fe alloys (with 2.0 to 8.0 wt. % Fe), precipitation-free structures were hardly observed even at for a growth velocity greater than 2.0 m/s. This may confirm that Al-Fe alloys have high resistance to the formation of segregation-free microstructure.

Microstructural investigations of some alloy

powders, such as Al-Cu and Al-Cr-Fe-Zr,[19] Al-Mg-Mn and Al-Li-Cr-Fe and Al-Cr-Fe,[20] have shown that segregation-free microstructures could be formed. It should be noted that Fe is not the main alloying element in the iron containing alloys listed above. The influence of Fe on segregation behaviour in those alloys may be insignificant compared to that of Cu, Mn, and Cr. The formation of segregation-free solid observed in those alloys may be strongly influenced by Cu, Mn, and Cr elements, which have larger partition coefficient values (k) and smaller values of freezing range DT compared to those of Fe.

Microstructure of Medium Size Powders (5-15 µm)

In powders with a diameter range of 5-15 µm, two groups of powders exhibiting different microstructures were observed. The first group exhibited microstructures consisting of both zone A and zone B morphologies (Fig 2a). Transition from zone A to zone B is easily recognised because of image contrast between these two zones. The size of zone A decreased with increasing powder particle size and this zone completely disappeared in powders larger than 10 mm, as illustrated in Figs 2a and 4a. In contrast, the size of zone B or microcellular structures increased with increasing powder particle size.

The second group of powders exhibited almost entirely zone B morphology. Nucleation sites were also observed to be on the surface of the melt droplet. After nucleation, growth of an a–Al front proceeded by a cellular mode and as the growth proceeded the cells became coarser. The cell spacings were observed to increase with increasing distance away from the nucleation site (nucleation site → zone B → zone C in Fig 4a). In some powders, globular intermetallic particles were observed in the region consisting of coarse cellular microstructures. The globular intermetallic particles were later identified as a globular cluster of randomly oriented MI (GCMI) phase. The microstructure consisting of coarse cells or dendrites with GCMI particles is designated here as 'zone C'.

Note that the GCMI particles are not single quasicrystals because the single quasicrystals exhibit SADPs with arrays of sharp Bragg spots, whereas the GCMI particles exhibit SADPs with a ring pattern. It has been reported that single quasi-crystals formed independently in the melt by homogeneous nucleation and diffusionless growth with rates of 1-2 m/s in melt-spun Al-Fe alloys.[8] Although nucleation of the GCMI particles occurs homogeneously, the growth mechanism and clustering of these particles are not understood yet.

Formation of Zone B

The microstructure consisting of both zone A and zone B can be explained as follows. The formation of zone A occurs following the mechanism given previously. While the planar a-Al front is advancing, the solid/liquid interface velocity decreases due to retardation caused by the latent heat released by recalescence. The planar front is not stable at velocities lower than the absolute velocity, V_{abs}.[21,22] The solidification front then changes from planar to cellular. In coarser powder particles with zone B microstructure initiated near a nucleation site (for example in Fig 4a), slow cooling rates inhibit latent heat removal. Therefore, low solid/liquid interface velocity causes planar front instability, which results in formation of cellular front. The interaction between the cellular front and the freely dispersed MI phase particles during the formation of zone B is such that the particles are pushed laterally or in other words, the cellular trunks penetrate into the space between the particles (Fig 3b). By this interaction, the MI particles are entrapped in the intercellular liquid that solidifies later at the end of solidification of a melt droplet.

Although a temperature rise in the intercellular liquid due to latent heat from recalescence is expected, the temperature may not be high enough to transform the MI to other crystalline phases. The MI phase is still detected in zone B of the as–atomised powders. The
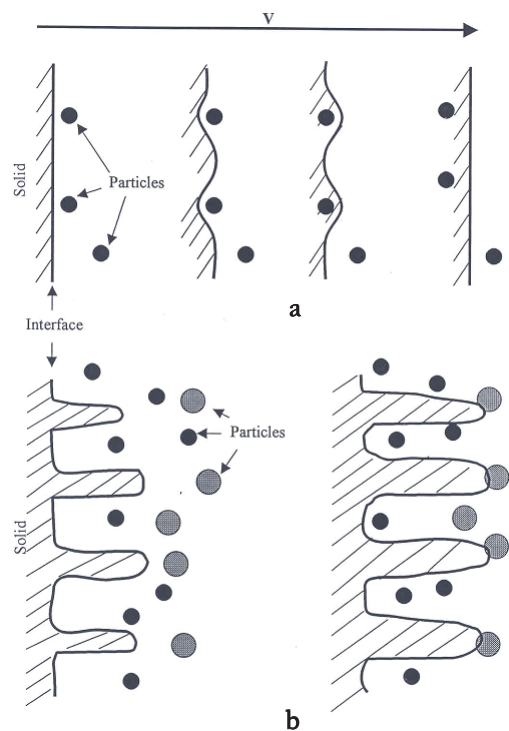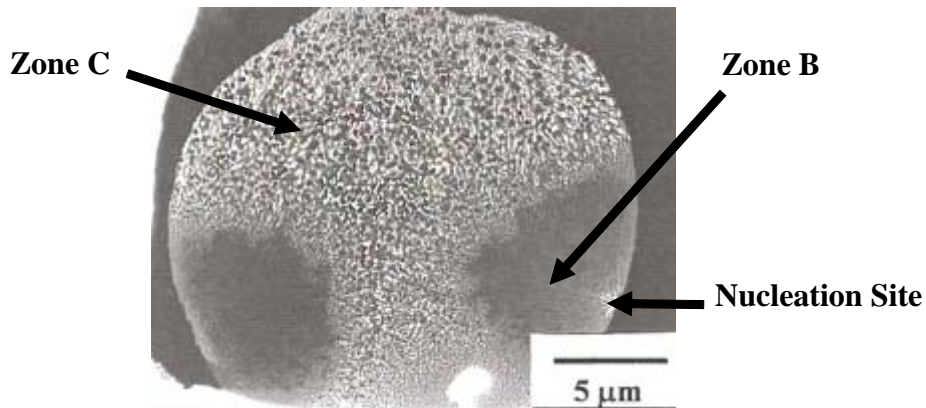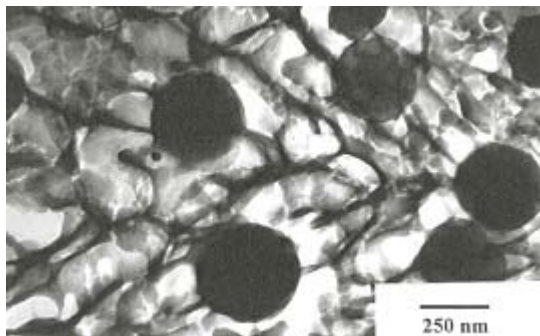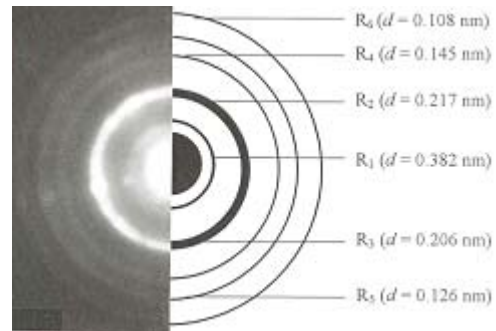

Fig 3. Schematic diagram showing interactions between particles and planar (a) and cellular (b) solidification fronts (adapted from Asthama *et al*[23]).

a   A poer particle of alloy X.

b   Zone C in an alloy X powder particle.

c   SADP of the GCMI particle in an alloy X powder particle.

Fig 4. Characteristics of powders with a diameter range > 15 mm.

crystalline phases are also expected to form and coexist with the entrapped MI phase particles in the intercellular regions because increased temperature in the intercellular liquid may promote the formation of crystalline phases.

Microstructure of Medium to Coarse Size Powders (> 15 μm)

The microstructures observed in medium to coarse size powders with diameters greater than 15 mm consisted of zone B and zone C (Fig 4). In alloy X powders, GCMI particles (also the zone C) were always observed at some distance away from the nucleation site for solidification of α–Al. The size and volume fraction of GCMI particles in zone C increased with increasing distance away from the nucleation site and also with increasing powder particle size. Nucleation sites for solidification of α–Al were observed to be on the surface of the melt droplet. This suggests that nucleation of α–Al in coarse powder particles may occur heteroge-neously. The growth of α–Al in coarse powders might start via a cellular mode and then changed to a dendritic mode.

In alloy Y powders, the globular particles exhibited SADPs with arrays of diffraction spots (Fig 5). The spots did not possess a long-range periodic translation order, but showed a crystallographically forbidden rotational fivefold symmetry. The SADPs in Fig 5 indicate that the globular particles are single icosahedral phase.

Formation of Zone C

The formation of zone C may also be explained by the interaction of the solidification fronts and the dispersed particles in the melt.[23-25] The dispersed globular particles in zone C are either GCMI or single icosahedral phase particles. Long before the interaction occurs, the globular particles have grown. The coarse cellular or dendritic fronts advancing with low velocities (indicated by large cell or dendrite spacings) push the large, freely dispersed globular particles ahead for some distance before the particles are entrapped by the solidifying fronts (Fig 3b).

The evidence of particle pushing during solidification is the presence of globular particles far away from the nucleation site for solidification of cellular or dendritic α–Al phase. It is interesting to note that the globular particle sizes are as large as the cellular or primary dendritic spacings. It is impossible for these particles to be entrapped in the smaller size intercellular/interdendritic regions. Therefore, the
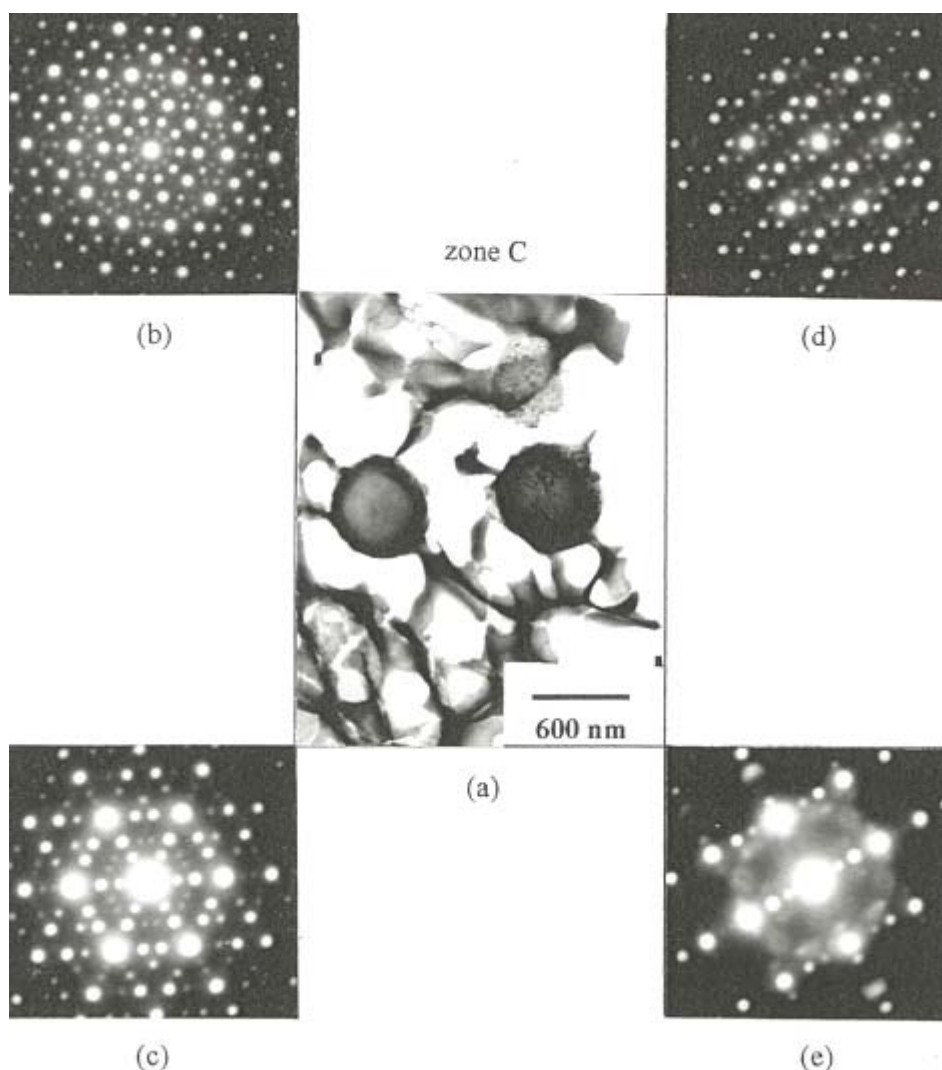
Fig 5. Globular particles and their SADPs in a coarse powder particle of alloy Y.

globular phase particles are dispersed and stuck to coarse cellular/dendritic networks (Figs 4b and 5a).
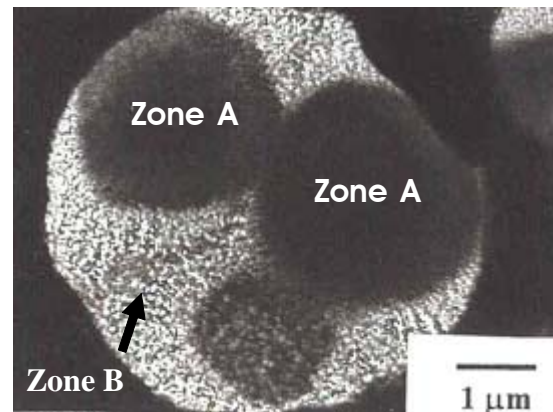
As in the intercellular liquid in zone B, increased temperature and solute content in the intercellular/interdendritic liquid in zone C are expected. The crystalline phases are likely to form in conjunction with the MI phase in the intercellular/interdendritic liquid. The continuous forms of metastable Al_6Fe phase were observed in the intercellular/interdendritic regions of coarse alloy X powders.
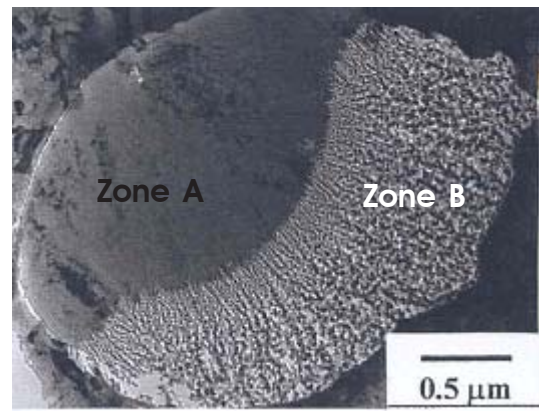
Nucleation in Melt Droplets

Powder microstructures usually exhibit a single nucleation site indicating that a powder particle is a single grain. A single grain powder particle occurs when growth kinetics are so rapid and there is insufficient time for a second nucleation event to occur before

recalescence has raised the temperature. The nucleation site is usually observed at the surface of the powder. This indicates that nucleation in a melt droplet occurs heterogeneously. Multiple grains in a single powder particle, as shown in Figs 2a, 4a and 6, resulting from multiple nucleation events in a melt droplet, were also observed. It may be implied that atomisation cannot totally split catalytic sites for nucleation down to one site per a melt droplet. Multiple grains in a single powder particle have also been observed in rapidly solidified Al-Fe-Cr-Zr powders.[19]
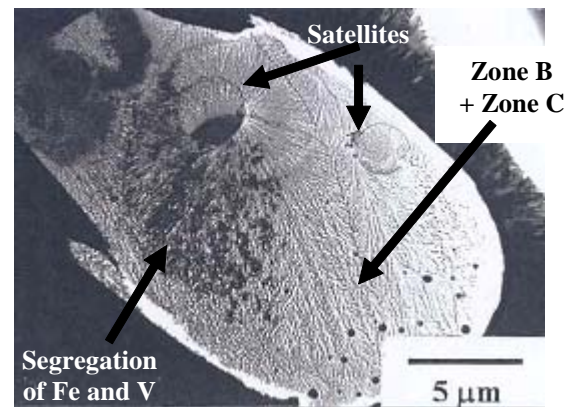
Grains formed from nucleation events occurring at nearly the same time were observed in some powders (Figs 2a, 4a and 6a). In these cases, the grain sizes were usually equal and the grains oriented symmetrically. Nuclei may have formed at different times resulting in the formation of grains with different sizes as clearly
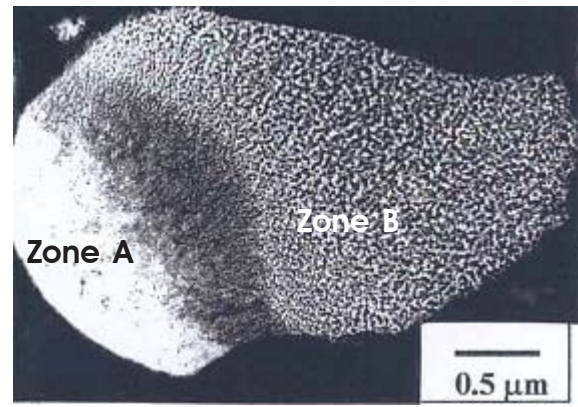
a   Alloy X.

a   Alloy X

b   Alloy X.

Fig 6. Examples of powders showing multiple nucleation sites.

b   Alloy Y.

Fig 7. Irregular shaped powders of alloys X and Y.

shown in the coarse irregular-shaped powder particle (Fig 6b).

Nucleation in large melt droplets may be triggered by a small satellite particle. Collision or impingement of smaller solidified powder particles on the larger molten or semi-molten droplets occurs during the atomisation process. The smaller powder particle, when impinging on a larger melt droplet, acts as a catalytic site for nucleation. Microcells of a larger powder particle grow and propagate from the surface of a smaller powder particle as can be clearly seen in Fig 6b.

Satellites, in the form of one powder particle attached to another powder particle, were not observed in fine size powders with the same diameters because solidification in a fine size powder particle occurs rapidly, before impingement by other fine size powder particles. Therefore, collisions involving solidified powder particles cannot generate satellites.

Competition between solidification and spherodisation

In general, spherical or nearly spherical shaped powder particles of aluminium or aluminium alloys are produced by gas atomisation. However, powders with irregular shape were observed in alloy X and alloy Y. (Fig 7). During atomisation processing, two different processes namely spherodisation and solidification occur. The irregularity of powder shape indicates that solidification of the melt droplets occurs very fast so that the melt had insufficient time to complete spherodisation. Irregular-shape powders were found in a wide range of powder sizes.

CONCLUSIONS

Microstructures of the gas-atomised Al-Fe-V and Al-Fe-V-Si alloy powders result from interactions between solidifying α–Al fronts with some forms of freely dispersed intermetallic particles in the melt ahead of the fronts. In fine size powders, microstructures indicate that the growing planar α–Al front engulfs the ultrafine MI particles freely dispersed in the melt. This results in formation of zone A microstructure in fine size powders. When the α–Al fronts are growing with a cellular mode, the ultrafine MI particles are pushed laterally or the cellular trunks penetrate into the space between the particles. This results in formation of zone B microstructure. In the case of coarse globular particles

distributing in the melt, the coarse cells may push the particles forward before entrapping them. This results in formation of zone C microstructure.

Apart from interactions between the solidified fronts and the freely dispersed particles in the melt, nucleation events and competition between solidification and spherodisation also influence powder characteristics. Multiple nucleation sites in one melt droplet would lead to formation of multiple grains in one powder particle. The melt droplet that solidifies very fast before spherodisation completes would result in formation of irregular-shaped powders.

ACKNOWLEDGEMENTS

REFERENCES

1. Jones H (1969/1970) Observation on a Structural Transition in Aluminium Alloys Hardened by Rapid Solidification. *Mater Sci Eng*, **5**(1), 1-18.
2. Chu MG and Granger DA (1990) Solidification and Microstructure Analysis of Rapidly Solidified Melt-Spun Al-Fe Alloys. *Metall Trans A* **21A**, 205-12.
3. Boettinger WJ, Bendersky LA, Schaefer RJ and Biancaniello FS (1988) On the Formation of Dispersoids during Rapid Solidification of an Al-Fe-Ni alloy. *Metall Trans A* **19A**, 1101-7.
4. Field RD, Zindel JW and Fraser HL (1986) The Intercellular Phase in Rapidly Solidified Alloys Based on the Al-Fe System. *Scripta Metall* **20**, 415-8.
5. Gremaud M, Carrard M and Kurz W (1990) The Microstructure of Rapidly Solidified Al-Fe Alloys Subjected to Laser Surface Treatment. *Acta Metall Mater* **38**, 2587-99.
6. Shechtman D and Swartzendruber LJ (1983) Metastable Phases in Rapidly Solidified Aluminium-Rich Al-Fe Alloys. *Mater Res Soc Symp Proc* **19**, 265-8.
7. Shechtman D, Blech I, Gratias D and Cahn JW (1984) Metallic Phase with Long-Range Orientational Order and No Translational Symmetry. *Phys Rev Lett* **53**, 1951-3.
8. Adam CM, Ramanan VRV and Skinner DJ (1986) Undercooled Phases in Aluminum –Iron Alloys. In: Undercooled alloy phases. (Collings, E. W., and Koch, C. C., eds.), The Metallurgical Society, Pennsylvania, 59-70.
9. Carrard M, Gremaud M and Pierantoni M (1991) Determination of the Structure of Intercellular Precipitates in Rapidly Solidified Al-Fe Alloys by Comparison with Al-Fe-Si Alloys. *Scripta Metall Mater* **25**, 925-30.
10. Kim DH and Cantor B (1994) Quasicrystalline and Related Crystalline Phases in Rapidly Solidified Al-Fe Alloys. *Phil Mag A* **69** (1), 45-55.
11. Skinner DJ and Okazaki K (1984) High Strength Al-Fe-V Alloys at Elevated Temperatures Produced by Rapid Quenching from the Melt. *Scripta Metall* **18**, 905-9.
12. Park WJ, Ahn S and Kim NJ (1994) Evolution of Microstructure in a Rapidly Solidified Al-Fe-V-Si Alloy. *Mater Sci Eng* **A189**, 291-9.
13. Srivastava AK and Ranganathan SA (1992) Novel Microstructure in a Rapidly Solidified $Al_{80}Fe_{10}V_4Si_6$ Alloy. *Scripta Met* **27**, 1241-5.
14. Wang JQ, Hao YY, Chang XC and Hu ZQ (1997) Formation and Structural Characterization of Al-Based Nanocomposite Materials. *Int. J. Non-Equilibrium Processing*, **10**, 83-92.
15. Urban K, Mayer J, Rapp M, Wilkens M, Csanady A and Fidler J (1986) Study on Aperiodic Crystals in Al-Mn and Al-V Alloys by Means of Transmission Electron Microscopy. *J de Phys Colloque C3* **47**, 465-75.
16. Bendersky LA, Biancaniello FS and Schaefer RJ (1987) Amorphous Phase Formation in $Al_{70}Si_{17}Fe_{13}$ Alloy. *J Mater Res* **2(4)**, 427-30.
17. Gill SC and Kurz W (1993) Rapidly Solidified Al-Cu Alloys-I. Experimental Determination of the Microstructure Selection Map. *Acta Metall Mater* **41(12)**, 3563-73.
18. Jones H (1988) The Critical Concentration for Formation of Segregation-Free Solid by Solute Trapping during Rapid Solidification from the Melt. *Mater Lett* **6**, 181-2.
19. Marshall GJ (1986) Microstructure of Rapidly Solidified Al Powder Alloys. In: Aluminum technology '86. (Sheppard, T., ed.), The Institute of Metals, London, pp. 679-88.
20. Sheppard T and Zaidi MA (1986) On the Observation of Partitionless Structures in Rapidly Solidified Al-Mg-Mn Alloy Powder. *Int. J Rapid Solidn* **2**, 199-204.
21. Trivedi R, Sekhar JA and Seetharaman V (1989) Solidification Microstructures near the Limit of Absolute Stability. *Metall Trans A* **20A**, 769-77.
22. Trivedi R and Kurz W (1986) Morphological Stability of a Planar Interface under Rapid Solidification Conditions. *Acta Metall* **34** (8), 1663-70.
23. Asthana R, Rohatgi PK and Tewari SN (1993) Pushing of Particles by a Solidification Front-Theory, Experiments and Relevance to Cast MMC'S. In: Microstructure formation during solidification of metal matrix composites. (Rohatgi, P. K., ed.), The Minerals, Metal & Materials Society, TMS, Warrendale, Pa, 11-28.
24. Fedorov OP (1992) Interaction between Growing Crystals and Inclusions in the Melt. *J Crys. Growth* **102**, 857-61.
25. Sekhar JA and Trivedi R (1990) Solidification Interface Configurations during the Processing of Particulate Composites. In: Solidification of metal matrix composites (Rohatgi P, ed.), The Minerals, Metals and Materials Society, 39-50.